2024 IEEE/ASME International Conference on Advanced Intelligent Mechatronics (AIM)
July 15-19, 2024. Boston, MA, USA

# Discrimination of Solid–Liquid Mixtures using a Multisensing System in a Peristaltic Mixing Conveyor that Imitates Intestinal Function

T. Tanno[1], I. Terayama[1], R. Adachi[1], and T. Nakamura[1], *Member, IEEE*

***Abstract*— Continuous mixing and conveying technology for solid–liquid mixtures is required in the manufacturing process of foods and medicines. To achieve this, we develop a peristaltic mixing conveyor that simulates the function of the human intestines. This device can mix and convey food and medicinal contents by inflating a rubber tube using air pressure. Currently, we are working on a system of content condition estimation using measurement data from the pressure and flow rate sensors installed in the device. However, these measurement methods use air supplied to the device as the measurement target, and the compressibility of air limits the conditions of contents that can be estimated. So, the generalizability of the estimation is low. In this study, a thin pressure-sensitive sensor is installed that can measure the mechanical responses of device contents due to mixing by the device. We also construct a multisensing system that combines conventional pressure/flow rate and pressing force measurements. Sensor data acquired when solid–liquid mixtures are fed into the device are applied to machine learning to distinguish the mixing ratios of the mixtures. Results show that the accuracy of mixing ratio discrimination is improved from 96.7% to 98.9% when pressure and flow rate data are combined with pressing force data. The results thus confirm the improved accuracy of content identification when pressure/flow rate and pressing force measurements are combined.**

## I. Introduction

Mixing and conveying technology for solid–liquid mixtures is required in a variety of fields, from familiar products such as food and medicine to the production of solid rocket fuel. Currently, separate devices are used for mixing and conveying, resulting in a batch process for the entire operation. This results in increased labor and other costs. In addition, the rotating mixer used for mixing generates large frictional and shear forces. These forces generate heat and shock, which can destroy the structure and organization of a mixture. Therefore, the driving conditions of the device are limited.

To solve these problems, we previously developed a peristaltic mixing conveyor that mimics the function of the human intestines [1]. The conveyor uses pneumatic artificial muscles for continuous mixing and conveying at a low shear force. This device can mix and convey powders or liquids by expanding an installed rubber tube with compressed air. To date, this device has succeeded in conveying powders [2] and highly viscous fluids and solid–liquid mixtures [3] and producing solid rocket fuel [4]. The human intestines function by an autonomous nervous system, which assesses bolus conditions from its mechanical/chemical stimuli sensed by the enteric nervous system and autonomous decentralized switching between segmental movements for mixing boluses and peristaltic movements for transporting mixtures. The mixing and conveying of contents such as solid–liquid mixtures and other fluids by this device change their mechanical properties such as their viscosity. Therefore, it is expected that efficient continuous mixing and conveying can be realized by sensing mechanical stimulation of the device contents like intestines in living organisms and that generates a driving pattern for the device based on the obtained content information. In the prior study, we applied sensing and autonomous decentralized control of the content mixture state by simulating the enteric nervous system [5]. We then constructed a sensing system to measure the pressure and flow rate of the air used to drive the device [6]. We also employed machine learning to estimate the mixing degree of powder and liquid [7]. Although a previous study [8] successfully estimated the mixing degree of solid rocket propellant packed in bags, the conditions of the contents by which the mixing degree was estimated by machine learning were limited. Estimation is particularly difficult when the order in which the contents are fed to the device or the arrangement of contents in the device is altered, and the current method has low generalizability in estimating the mixing degree.

In this study, a thin pressure-sensitive sensor that can measure the pressing force between the rubber tube of the device and the device contents is introduced to improve generalizability in estimating the content mixing degree in the peristaltic mixing conveyor. This sensor can sense the tactility of the contents, which changes in the process of mixing that. By combining pressure/flow rate measurement with pressing force measurement, the pressing force measurement complements estimation under content conditions that are difficult to estimate previously. In this way, we aim to improve the generalizability of the estimation using the multisensing method. We conducted an experiment by placing bagged solid–liquid mixtures in the device. The measured values of pressure, flow rate, and pressing force were input into a machine learning model to distinguish the mixing ratios, and the effect of multi-mediatization by the introduction of pressing force measurement is studied.

The remainder of this paper is organized as follows. Section 2 summarizes the peristaltic mixing conveyor and content sensing system. Section 3 describes the experiments for acquiring sensor data used in mixing ratio classification. Section 4 describes mixing ratio discrimination by machine learning, and Section 5 provides a summary and future prospects.

The contributions of this paper are showed as follows.

- The mixing ratio of solid-liquid mixtures packed in bags was successfully identified using machine learning based on data obtained from pressure/flow rate sensors and thin pressure sensitive sensors installed on a peristaltic mixing conveyor.
- Multisensing of pressure/flow rate and pressing force measurements was suggested to be effective for content state estimation during mixing when the difference of deformation behavior of the rubber tube was difficult to observe.

[1] T. Tanno, I. Terayama, R. Adachi, and T. Nakamura are with the Faculty of Science and Engineering, Department of Precision Mechanics, Chuo University, 1-13-27 Kasuga, Bunkyo-ku, Tokyo 112-8551, Japan (e-mail:t_tanno@bio.mech.chuo-u.ac.jp).

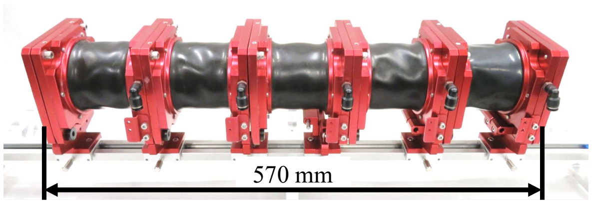


(a)

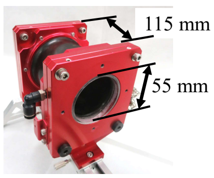


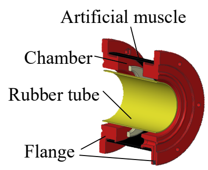


(b) (c)

Fig. 1 (a) Overall view, (b) The single unit appearance, and (c) sectional view of Peristaltic Continuous Mixing Conveyor

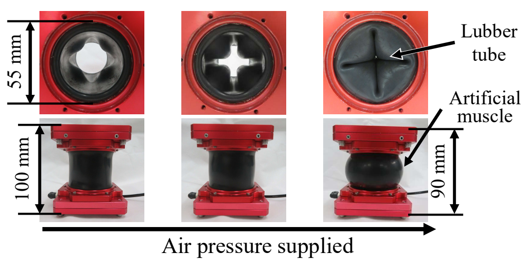


Fig. 2 Driving of the single unit

## II. Peristaltic Mixing Conveyor and Sensing System

### *A. Device Overview*

This section describes the structure of the peristaltic mixing conveyor. Fig. 1 presents an overall view of the device and the appearance and cross-sectional view of each unit. This device is a unit configuration, and each unit of which can be driven independently to imitate intestinal function. The intestines perform segmental operations in mixing food masses and digestive juices and performs peristalsis to convey the mixtures. These movements can be reproduced by the device by designating the unit in which air pressure is applied. Each unit consists of an axial fiber-reinforced pneumatic artificial muscle (hereinafter “artificial muscle”), a rubber tube, and flange. Fig. 2 shows the way the device is driven. The inside of the tube is closed by the application of air in the chamber space between the rubber tube and artificial muscle. Simultaneously, the artificial muscle expands radially and contracts axially to facilitate the occlusion of the canal and the mixing and conveying of the contents. Each unit is equipped with pressure and flow rate sensors to measure the chamber pressure and supply and exhaust flow rates, respectively. The volume and viscosity of the contents can be detected from these sensor values [6], and applied machine learning can estimate the mixing degree of the contents [7].

### *B. Challenges related to Pressure and Flow Rate Measurement and the Proposal of Multi-Sensing Method*

Pressure and flow rate measurements of the contents of peristaltic mixing conveyors have generalizability problems when the mixing degree is estimated. Based on pressure and flow rate values, these measurement methods detect differences in the volume and flowability of the residual

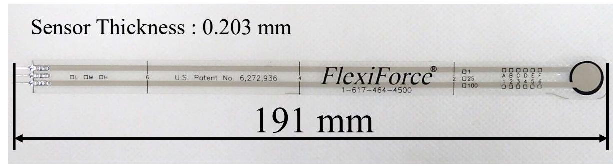


(a)

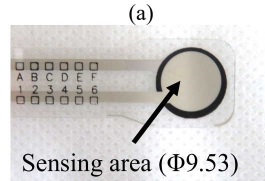


(b)

Fig. 3 Thin Pressure sensitive sensor
(a) Overall view (b) Sensing area

contents in the rubber tube as mixing progresses. However, these changes due to mixing may be small depending on the fed amount and order of mixed materials, making it difficult to detect the mixing degree. Therefore, pressure and flow rate measurements alone limit the content conditions under which the mixing process can be assessed, and the generalizability of the mixing degree estimation is low.

In this study, we construct a multisensing environment that combines pressure/ flow rate with another sensor information. Specifically, we develop a sensing system that has high estimation generalizability, which is accomplished by supplementing the estimation of mixing degree under the content conditions (previously difficult to determine) with another sensor information. In a previous study, a triaxial acceleration sensor [9] was introduced to measure the deformation behavior of the rubber tube in the device when air was applied to the device. However, due to the significant effects of noise, discriminating the contents from the measured values proved difficult.

With the introduction of a sensor that directly measures the mechanical response of the rubber tube in the device when it supplies a pressing force against the device contents, changes in the mechanical properties (such as viscosity and liquidity) of the contents during mixing can be directly measured. As a method for measuring contact force with objects, tactile sensors such as piezoresistive sensors can be used. They have been developed for tactile measurements in industrial robots and cooperative work robots [10]–[12]. Typically, they are sheets that can be applied to robotic skin and can be flexibly deformed to fit the object to which they are attached. In our case, to measure the pressing force in the mixing conveyor, a sensor that can be attached to the surface of the rubber tube is required. The thin pressure-sensitive sensor is flexible in sheet form and can be deformed to fit the rubber tube. It is thus suitable for mounting on our device. In addition, because this sensor is thin, conveying of the contents in the device are not obstructed even the sensor is installed on the rubber tube. Therefore, it can directly measure the contents without interfering with mixing and conveying. By the introduction of this sensor, we construct a multisensing environment that combines pressure and flow rate measurements that target the compressed air which is supplied in the chamber of the device and a pressing force measurement that does not use inclusions. The goal is to improve generalizability in content state estimation.

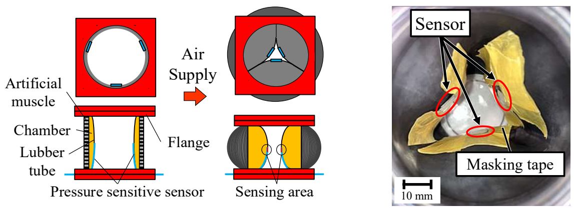


(a) (b)

Fig. 4 Sensor mounting on the single unit of the device
(a) Mounting concept (b) Attached sensors

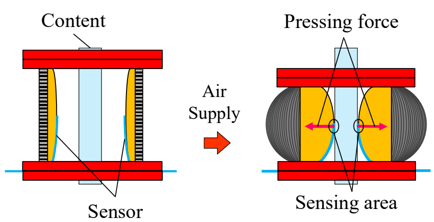


Fig. 5 Pressing force measurement

### C. *Installation of Thin Pressure Sensitive Sensor*

A thin pressure-sensitive sensor was mounted on a rubber tube in a device. This section describes the mounting method for the sensors and the pressing force measurement. Fig. 3(a) shows the thin pressure-sensitive sensor (Tekscan FlexiForce A201). When a load is applied to the sensing area, as shown in Fig. 3(b), the resistance value decreases due to the piezoresistive effect, and the contact pressure is measured. When compressed air is applied to the device, the rubber tube is occluded at three equally spaced locations in the circumferential direction. Three sensors are mounted on the surface of the rubber tube to establish a sensing area at each of the three blockage points (Fig. 4). When the device operates after being placed contents, as shown in Fig. 5, the sensing area makes contact with the contents as the rubber tube presses against them to measure the pressing reaction force. In this study, as an initial study of mixing state estimation by a multisensing system including pressing force measurement, a solid–liquid mixture packed in a plastic bag was fed into a device mounted with pressure-sensitive sensors, and the chamber pressure, supply and exhaust flow rates, and pressing force were measured. The measurements were then used as input variables for machine learning to discriminate the mixing ratios of the mixtures. The effect of the pressing force measurement on the accuracy identification of contents was then assessed.

## III. Solid-Liquid Mixture Measurement Experiment

An experiment was conducted in which bagged solid–liquid mixtures were fed into a single unit of a device mounted with three thin pressure-sensitive sensors to measure the chamber pressure, supply/exhaust flow rates, and pressing force.

### A. *Experimental Method*

Fig. 6 shows the experimental environment, where the device was installed vertically for the experiment. Compressed air was used to drive the device and was supplied from an air compressor into the chamber through the supply-side solenoid valve (SMCVX210AGA) and was exhausted through the exhaust-side solenoid valve. The applied pressure of the compressed air was set to 60 kPa by a regulator. A pressure sensor (CKD PPX-R01PH-6M) to measure the chamber pressure and a flow rate sensor (SMC PFM750-C6-C) to

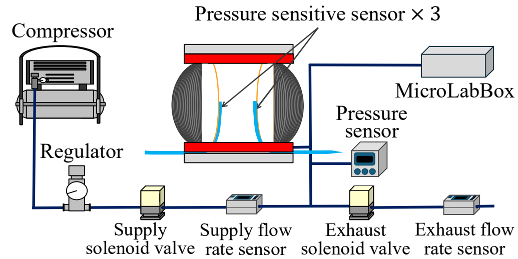


Fig. 6 Experimental environment

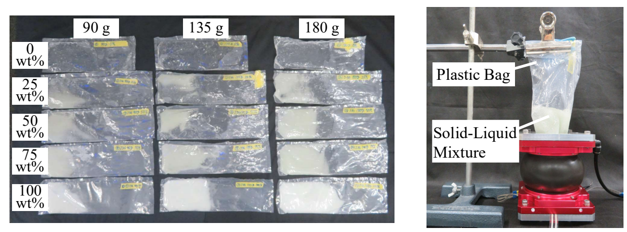


(a) (b)

Fig. 7 Solid-Liquid mixtures
(a) Bagged samples (b) Insertion method into the device

measure the supply and exhaust flow rates were installed on the pneumatic circuit. The opening/closing signal transmission of the solenoid valve and the acquisition of sensor data were performed using Micro Lab Box (dSPACE), and the sampling period was set to 0.05 s. In this experiment, the device was driven for 10 s per cycle (5 s each of supply and exhaust). The device drove ten cycles of driving for each solid–liquid mixture sample, which was considered as one experiment.

In this experiment, mixtures of glass beads (particle sizes of 425–600 μm, hereinafter "powder") and aqueous sodium polyacrylate solution (17.2 Pa・s, hereinafter "liquid") packed in low-density polyethylene bags (300 × 90 × 0.08 mm) were used as device contents. To perform clustering of the mixing ratio of the mixture using the acquired sensor data, five mixing ratio conditions were established with the mass ratios of powder-to-mixture set to 0, 25, 50, 75, and 100 wt%, respectively. To investigate the effects of the total mixture amounts on the discrimination accuracy, three total amount conditions of 90, 135, and 180 g were set, and the samples were prepared under each total amount condition at five mixing ratios (Fig. 7 (a)). The samples were placed in the rubber tube suspended from above the device (Fig. 7 (b)).

### B. *Acquired Experimental Data*

In this experiment, for each cycle of device operation, the chamber pressure was obtained from the pressure sensor, the flow rate values of air supply and exhaust from the flow rate sensors, and the pressing force values from three pressure-sensitive sensors. A 2nd-order Butterworth low-pass filter (cut-off frequency: 1 Hz) was applied to the measured pressing force data using MATLAB (ver. 2023a, MathWorks) to reduce noise.

### C. *Experimental Result*

Fig. 8 shows the time-series data per cycle averaged over 18 cycles for each of the five mixing ratio conditions based on the acquired data of chamber pressure, air supply and exhaust flow rates, and pressing force. For the total mass conditions, the upper graph is 90 g, the middle 135 g, and the lower 180 g. The

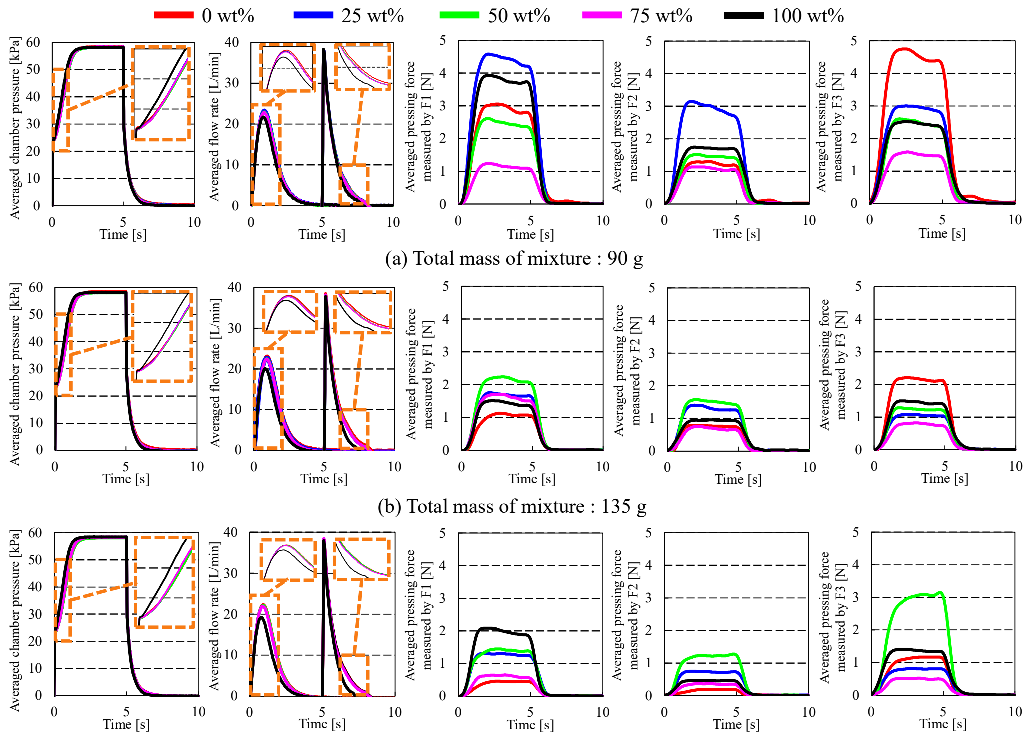


(a) Total mass of mixture : 90 g

(b) Total mass of mixture : 135 g

(c) Total mass of mixture : 180 g

Fig. 8 The time-series data of averaged chamber pressure, flow rate, and pressing force for each total mass condition of mixtures.

graphs show (from left to right) the chamber pressure, air supply and exhaust flow rates, and pressing force for each total mass condition. The pressing force is a time-series graph averaged from each of the three sensors (F1, F2, and F3) mounted on the device. Fig. 8 shows the difference in sensor values based on the mixing ratio at 2 s after the start of supplying air for the chamber pressure, 1 to 4 s after the start of supplying air and 3 s after the start of exhaust for the flow rate. In the graphs for pressing force, the difference in measurement values based on the mixing ratio was clearly observed at 6 s from the rise until the fall of the graph.

## IV. Mixing Ratio Discrimination by Machine Learning

Next, the acquired sensor data were input into a machine learning model to perform multiclustering of the five mixing ratios. First, the mixing ratios of the mixture (0, 25, 50, 75, and 100 wt%) were labeled for four types of sensor data (chamber pressure, supply flow rate, exhaust flow rate, and pressing force). Labeled data were used as the ground truth for machine learning. Feature values were extracted from time series data of each sensor and 11 datasets were created with different numbers and combinations of sensors. Each dataset was then fed into a classifier to compare discrimination accuracy. MATLAB was used for data processing.

### A. *Input Variables for Machine Learning*

This section describes the feature value extraction of sensor data input to the machine learning model. The feature values per cycle were pressure value at 0.8 s after supply started for chamber pressure, integrated value for 5 s of the supply and exhaust sections in flow rate, and time integrated value of the measurement value for 10 s per cycle in pressing force. Each feature value was extracted over 18 cycles. For each total mass condition (90, 135, and 180 g), 11 datasets were created: four datasets using each sensor data individually and seven datasets under different numbers and combinations of sensors. Table 1 lists the datasets and numbers of input variables.

Table 1 Variables for each dataset
(Pa : Chamber pressure, FRin : Supply flow rate,
FRout : Exhaust flow rate, F : Pressing force)

| No. | 1 | 2 | 3 | 4 | 5 | 6 |
|---|---|---|---|---|---|---|
| Data Set | Pa | FRin | FRout | F | Pa +FRin | Pa +FRout |
| Variables | 1 | 1 | 1 | 3 | 2 | 2 |
| No. | 7 | 8 | 9 | 10 | 11 | |
| Data Set | FRin +FRout | Pa+FRin +FRout | F +Pa | F +FRin | F +FRout | |
| Variables | 2 | 3 | 4 | 4 | 4 | |

### B. *Machine Learning Model*

The k-nearest neighbor algorithm (k-NN) was used as a machine learning model to discriminate the mixing ratios of mixtures. Thirty-three datasets were entered into the classifier, and the mixing ratios of the mixtures were discriminated.

k-NN is a learning model that classifies unknown data by calculating the distance between known training data and unknown data plotted in vector space. It then extracts k training data in the neighborhood of the unknown data and the unknown data are classified by majority voting of the extracted data. k-NN is non-parametric learning model and can be applied universally to any data. Therefore, it is suitable for clustering with integrated different sensor data as this study. In this study, the amount of neighborhood data extracted was 1 (k = 1), and Euclidean distance was used for distance calculations. A five-fold cross validation was also conducted.

Table 2 Discrimination accuracy for each dataset using by k-NN.

| Data Set | Pa | FRin | FRout | F | Pa +FRin | Pa +FRout | FRin +FRout | Pa+FRin +FRout | F +Pa | F +FRin | F +FRout |
|---|---|---|---|---|---|---|---|---|---|---|---|
| 0 wt% | 38.9% | 44.4% | 50.0% | 100% | 61.1% | 66.7% | 94.4% | 72.2% | 100% | 94.4% | 100% |
| 25 wt% | 38.9% | 72.2% | 33.3% | 77.8% | 83.3% | 38.9% | 100% | 77.8% | 94.4% | 94.4% | 94.4% |
| 50 wt% | 27.8% | 61.1% | 61.1% | 88.9% | 61.1% | 66.7% | 83.3% | 83.3% | 88.9% | 83.3% | 100% |
| 75 wt% | 66.7% | 55.6% | 100% | 88.9% | 72.2% | 100% | 100% | 100% | 94.4% | 83.3% | 94.4% |
| 100 wt% | 100% | 100% | 100% | 77.8% | 100% | 100% | 94.4% | 100% | 100% | 100% | 100% |
| Total | **54.4%** | **66.7%** | **70%** | **90%** | **75.6%** | **74.4%** | **95.6%** | **96.7%** | **95.6%** | **98.9%** | **97.8%** |

(a) Total mass of mixture : 90 g

| Data Set | Pa | FRin | FRout | F | Pa +FRin | Pa +FRout | FRin +FRout | Pa+FRin +FRout | F +Pa | F +FRin | F +FRout |
|---|---|---|---|---|---|---|---|---|---|---|---|
| 0 wt% | 22.2% | 100% | 100% | 83.3% | 100.0% | 100% | 100% | 100% | 83.3% | 94.4% | 100% |
| 25 wt% | 44.4% | 72.2% | 100% | 44.4% | 83.3% | 100% | 100% | 100% | 66.7% | 66.7% | 94.4% |
| 50 wt% | 55.6% | 88.9% | 72.2% | 66.7% | 77.8% | 94.4% | 100% | 100% | 77.8% | 72.2% | 100% |
| 75 wt% | 38.9% | 83.3% | 77.8% | 72.2% | 66.7% | 94.4% | 100% | 100% | 66.7% | 77.8% | 94.4% |
| 100 wt% | 100% | 100% | 100% | 83.3% | 100% | 100% | 100% | 100% | 100% | 100% | 100% |
| Total | **46.7%** | **88.9%** | **90%** | **63.3%** | **92.2%** | **97.8%** | **100%** | **100%** | **78.9%** | **82.2%** | **83.3%** |

(b) Total mass of mixture : 135 g

| Data Set | Pa | FRin | FRout | F | Pa +FRin | Pa +FRout | FRin +FRout | Pa+FRin +FRout | F +Pa | F +FRin | F +FRout |
|---|---|---|---|---|---|---|---|---|---|---|---|
| 0 wt% | 66.7% | 100% | 33.3% | 94.4% | 100% | 72.2% | 100% | 100% | 100% | 100% | 100% |
| 25 wt% | 38.9% | 72.2% | 61.1% | 94.4% | 72.2% | 50.0% | 94.4% | 94.4% | 83.3% | 94.4% | 94.4% |
| 50 wt% | 55.6% | 88.9% | 61.1% | 100% | 88.9% | 38.9% | 94.4% | 100% | 100% | 100% | 100% |
| 75 wt% | 72.2% | 83.3% | 83.3% | 66.7% | 94.4% | 88.9% | 100% | 100% | 88.9% | 88.9% | 94.4% |
| 100 wt% | 100% | 100% | 100% | 88.9% | 100% | 100% | 100% | 100% | 100% | 94.4% | 100% |
| Total | **66.7%** | **88.9%** | **64.4%** | **87.8%** | **92.2%** | **81.1%** | **97.8%** | **98.9%** | **94.4%** | **96.7%** | **96.7%** |

(b) Total mass of mixture : 180 g

Over 75 %  Under 50 %  Maximum Accuracy

### C. *Discrimination Result*

Table 2 shows the discrimination accuracies of all datasets under each total mass condition. The second through sixth rows of this table show the discrimination rates for each mixing ratio condition, and the seventh row shows the discrimination accuracies for all mixing ratios. The dataset with the highest overall discrimination accuracy under each total mass condition is shown in red. In the datasets in which each of the four sensors was used alone (Pa, FRin, FRout, and F), conditions with of less than 50% and more than 75% identification accuracy are given in blue and yellow, respectively.

When the total mass was 90 g and only pressure and flow rate data were used, the correct response rate was lower for mixtures with low powder content (0, 25, and 50 wt%) than with high powder content (75 and 100 wt%). However, when only the pressing force data were used, all mixing ratios could be discriminated with an accuracy of more than 75%. The combination of pressing force and flow rates resulted in a maximum discrimination rate of 98.9%.

When the total masses were 135 g and 180 g, the pressure data discriminated with high accuracy when the content was only powder (100 wt%), whereas the other mixture ratios were discriminated at a maximum of only 72.2%. In the flow rate data, the mixtures with less powder components were identified accurately, and the overall accuracy was approximately 90%. When pressing force data were used alone, the correct response rate was less than 70% for some mixing ratios, and the overall accuracy was lower than that when the total mass was 90 g. The maximum accuracy for a total mass of 135 g was 100% when using the dataset combined pressure and exhaust flow rates. The maximum accuracy for a total mass of 180g was 98.9% when using the dataset combined chamber pressure, supply, and exhaust flow rates. Therefore, when the total masses were 135 g and 180 g, only the pressure and flow rate data could be used to identify the mixing ratio with sufficiently high accuracy without including the pressing force measurements.

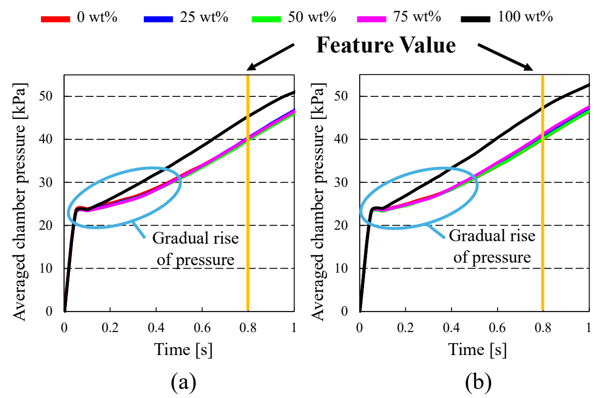


Fig. 9 The time-series data of chamber pressure. Total masses of mixtures are (a) 135 g and (b) 180 g, respectively.

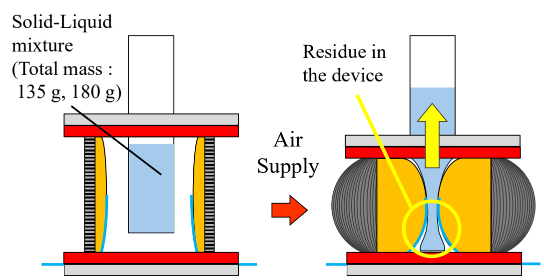


Fig. 10 The state of the device when total masses of mixtures are 135 g and 180 g.

Based on the previous, the combination of pressure and flow rates alone could not accurately discriminate some of the mixing ratios of solid–liquid mixtures when the amount of the mixture was small, and the discrimination rate was improved by combining the pressure and flow rates with the pressing force measurement. However, when the total mass of the mixture was increased, highly accurate identification was possible only by measuring the pressure and flow rates. Accordingly, the introduction of the pressing force measurement could be confirmed as improving the identification accuracy when the total mass of the mixture was small.

### D. *Discussion*

(a) Effects on pressure/flow rate measurement due to differences in the total mass of the mixture

Table 2 shows that discrimination by pressure and flow rate data yielded a low accuracy for mixtures with a low powder ratio when the mixture mass was 90 g. This was because the mixture with low powder content had high liquidity. Highly fluid objects were forced out of the device when the lubber tube was closed. Therefore, when a mixture with a low powder ratio was put into the device, nearly all the contents were forced out, where the differences in the deformation behaviors of the rubber tube due to different mixing ratios were not readily apparent.

When the total masses were 135 g and 180 g, pressure data discriminated only powders with high accuracy (100 wt%), but the discrimination rate for other mixing ratios containing liquids was only approximately 70% at maximum. This was because the increased total mass of the mixture increased the liquid mass in the mixture, and the stiffness of the contents decreased. Compared to when the content was only powder, the mixture containing liquid exhibited greater cushioning, and the rubber tube expanded more slowly. Consequently, the pressure value increased slowly from 0.1 to 0.5 s after supply of compressed air started regardless of the mixing ratio, as shown as Fig. 9. Therefore, we observed no clear difference in the pressure values after 0.8 s from air supply start in the mixing ratios except for that of 100 wt%. However, the flow rate data accurately identified mixtures with low powder content at a discrimination rate of approximately 90% with all mixing ratios. This was because when the amount of mixture was increased, the highly fluid mixture was not totally expelled after being forced by the rubber tube, and some remained in the device (Fig. 10). Differences in the properties of the residues such as fluidity and viscosity according to the mixing ratio affected the ease at which the contents were forced by the rubber tube, and it was hard to observe differences in the flow rate of air in the chamber.

(b) Effects on pressing force measurement due to differences in the total mass of the mixture

When the total mass was 90 g, discrimination using pressing force data resulted in a classification accuracy of greater than 75% for all mixing ratios. This was because the mixture adhered to the inside of the bag at the blockage point when the rubber tube was closed. The number of grains of powder contained in the adhered mixture differed depending on the mixing ratios, and the difference in the number of grains was reflected in the pressing force values.

When the total masses were 135 g and 180 g, the discrimination rate was less than that for a mass of 90 g for some mixing ratios. This was because the liquid mass in the mixture increased with the total mass, and the effects of the fluidity and cushioning properties of the liquid were more easily reflected in the pressing force values. These effects made it difficult to observe the difference in pressing force depending on the mixing ratios.

(c) Effects of introducing the pressing force measurement

In this experiment, when the total mass of the mixture was low, conditions were present that made it difficult to classify the mixing ratios with high accuracy when only measuring the pressure and flow rate. This was due to the effects of the flowability of the contents. However, the pressing force measurement could capture differences in the mechanical properties of the mixture depending on the mixing ratio from the small amount of adhered mixture to the bag. Still, as the total mass increased, the mixing ratio could be discriminated with high accuracy from the difference in flow rate with the deformation of the rubber tube. By contrast, the discrimination by pressing force measurement decreased the accuracy due to the effects of the flowability and cushioning of the liquid. Therefore, when the volume of the contents was low or when the contents were highly fluid under conditions in which differences in the deformation of the rubber tube were difficult to detect, the multisensing method of pressure/flow rate and pressing force measurement was effective in content state estimation.

## V. Conclusion

In this study, thin pressure-sensitive sensors were mounted on a rubber tube of the peristaltic mixing conveyor to improve the generalizability of content state estimation. Bagged solid–liquid mixtures were placed in the device under different mixing ratios and total content masses, and the sensor values of chamber pressure, supply/exhaust flow rates, and pressing force were obtained during device operation. The acquired sensor data were applied to machine learning to discriminate the mixing ratios of mixtures. Results showed that the identification accuracy was improved by the multimodal sensing system that combines pressure/flow rate and pressing force measurement under a low total mixture mass.

In a future work, we will mount thin pressure-sensitive sensors on multiple units of the device and attempt to detect the mixing process of solid–liquid mixtures using the multisensing method developed in this study. Simultaneously, we will experiment under different conditions such as the amount of mixture and input sequence of liquid and powder to verify the generalization performance of the multisensing system on mixing process detection.

## References


[1] W. A. A. Kunze and J. B. Furness, "The enteric nervous system and regulation of intestinal motility," Annual review of physiology, Vol. 61, No. 1, 1999, pp. 117-142.

[2] S. Yoshihama, et al., "Powder Conveyance Experiments with Peristaltic Conveyor using a Pneumatic Artificial Muscle," in Proc. of the 2016 IEEE/ASME International Conference on Advanced Intelligent Mechatronics (AIM2016), Banff, AB, Canada, Jul., 2016, pp. 1539-1544.

[3] S. Yoshihama, et al., "Mixing of solid propellant by peristaltic pump based on bowel peristalsis," in Proc. of the 2015 IEEE/RSJ International Conference on Intelligent Robots and Systems (IROS2015), Hamburg, Germany, Sept., 2015, pp. 3862-3868.

[4] K. Ashigaki, et al., "Considering mixing process of rocket solid propellant using mixing transport device simulating peristaltic movement of intestinal tract," in Proc. of the 2018 7th IEEE International Conference on Biomedical Robotics and Biomechatronics (Biorob2018), Enschede, Netherlands, Aug., 2018, pp. 1291-1296.

[5] D. Matsui, S. Oshino, I. Terayama, R. Nishihama, M. Okui, and T. Nakamura, "Proposal of a decentralized peristaltic movement generation based on the actual intestine and verification by content transfer experiment," in Proc. of the 2022 IEEE/SICE International Symposium on System Integration (SII2022), Narvik, Norway, Jan., 2022, pp. 65-70.

[6] K. Wakamatsu, D. Hagiwara, et al. "Content Detection for Continuous and Efficient Production of Solid Rocket Fuel by Peristaltic Mixer," 2020 IEEE/SICE International Symposium on System Integration (SII2020), Honolulu, HI, USA, Jan., 2020, pp. 471-476.

[7] K. Wakamatsu, et al. "Mixing State Estimation of Peristaltic Continuous Mixing Conveyor with Distributed Sensing System Based on Soft Intestine Motion", in Proc. of the 2020 3rd IEEE International Conference on Soft Robotics (RoboSoft2020), New Haven, CT, USA, May, 2020, pp. 208-214.

[8] I. Terayama, S. Oshino, R. Nishihama, M. Okui, R. Adachi and T. Nakamura, "Construction of Motion Mode Switching System by Machine Learning for Peristaltic Mixing Conveyor Based on Intestinal Movement," in IEEE Access, doi: 10.1109/ACCESS.2024.3366457.

[9] S. Oshino, K. Wakamatsu, et al. "Construction of Distributed Sensing System for Peristaltic Continuous Mixing Conveyor Imitating Intestines: Internal State Measurement Using Accelerometer," in Proc. of the IEEE International Conference on Advanced Intelligent Mechatronics (AIM2021), Delft, Netherlands, Jul., 2021, pp. 86-92.

[10] Min Jin Yang, et al. "Touch Classification on Robotic Skin using Multimodal Tactile Sensing Modules," in Proc. of the 2023 IEEE International Conference on Robotics and Automation (ICRA2023), London, UK, May, 2023, pp.9917-9923.

[11] Markus Fritzsche, Jose Saenz, and Felix Penzlin, "A large scale tactile sensor for safe mobile robot manipulation," in Proc. of the 2016 11th ACM/IEEE International Conference on Human-Robot Interaction (HRI2016), Christchurch, New Zealand, Apr., 2016, pp. 427-428.

[12] Xinkai Xia, et al. "Development of the Flexible Tactile Sensor for Safe Human-Robot Interaction," in Proc. of the 2022 12th International Conference on CYBER Technology in Automation, Control, and Intelligent Systems (CYBER2022), Baishan, China, Jul., 2022, pp. 764-768.